Characteristics of a high energy $\mu^+\mu^-$ collider based on electro-production of muons

William A. Barletta *,+, Andrew M. Sessler ++

Lawrence Berkeley Laboratory, Berkeley, CA, USA

We analyze the design of a high energy $\mu^+\mu^-$ collider based on electro-production of muons. We derive an expression for the luminosity in terms of analytic formulae for the electron-to-muon conversion efficiency and the electron beam power on the production target. On the basis of studies of self-consistent sets of collider parameters under "realistic" ("optimistic") assumptions about available technology with beam cooling, we find the luminosity limited to 10^{27} cm^{-2} s^{-1} (10^{28} cm^{-2} s^{-1}). We also identify major technological innovations that will be required before $\mu^+\mu^-$ colliders can offer sufficient luminosity (10^{30} cm^{-2} s^{-1}) for high energy physics research.

1. Introduction

Many physicists consider that the recent determinations of lower bounds for the mass of the top meson reinforce arguments that a Standard Model Higgs should have a mass less than twice the mass of the Z. This consideration has led to renewed interest in muon colliders as an ideal means of probing the mass range from m_Z to $2m_Z$. More generally, a muon collider with center-of-mass energy in the range of 200 to 400 GeV has the potential to produce very large numbers of Higgs particles because of the enhanced (vis a vis electrons) muon coupling to the Higgs. For such a collider to have maximum discovery potential the luminosity should be $\geq 10^{30}$ cm^{-2} s^{-1} [1]. As the muon is an unstable particle, the muons must be generated as secondary beams from either a proton beam or an electron beam striking a production target. The muons that emerge from the target must then be gathered and accelerated rapidly to high energy, at which point they can be injected into a storage ring collider with superconducting magnets.

This paper analyses the possibility of using electro-production to generate the muon beams. The chief advantage of producing the muons with an electron beam from a high energy, linear accelerator is that the bunches of muons are naturally formed with a short bunch length (< 1 cm) for acceleration to the desired high energy in a subsequent linear accelerator. As the muons will retain their short bunch length in the collider, a low β interaction region can be employed. This scheme is illustrated in Fig. 1.

2. Electro-production

Muons can be produced by an electron beam via two classes of processes, 1) $\mu^+\mu^-$ pair production and 2) photo-production of π's and K's, which subsequently decay into muons. It is known experimentally [2] that the cross-section for pair production is much more than an order of magnitude greater than that for process (2). Consequently, in the discussion that follows we will consider only pair production.

To estimate the muon pair production from an electron beam of energy, E_e, incident upon a thick target of atomic number Z, one can use the expression from Nelson [3] based on approximation A of shower theory. F is number of muons per electron produced at an angle $\geq \phi$ with respect to the incident electron beam:

$$\frac{\mathrm{d}F}{\mathrm{d}E}(E_e, E, \phi)$$

$$= \frac{1}{(2\pi)^2}\frac{m^2}{\mu^2}\frac{0.572 E_e \eta}{\mu^2 \ln(183Z^{-1/3})}2\ln(\gamma_\mu)$$

$$\times \left\{(1-\nu^2) - 0.33\left[1 - 4\nu^3(1-0.75\nu)\right]\right.$$

$$\left.\times \eta[1+\gamma^2]\right\}, \tag{1}$$

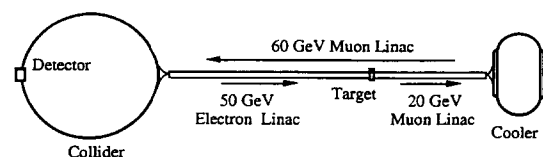where m = electron mass, μ = muon mass, E = energy of

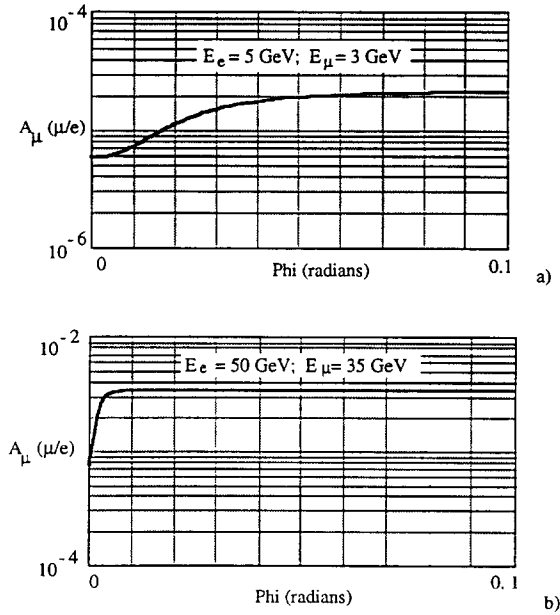Fig. 1. The scheme for a μ^+/μ^- collider using electro-production.

Fig. 2. Number of μ pairs per e^- accepted at an angle $\leq \phi$ for (a) a 5 GeV electron beam with $E_\mu = 3$ GeV and (b) a 50 GeV electron beam with $E_\mu = 35$ GeV.

the muon at the production target, $\gamma_\mu = E/\mu$ at the production target, $\nu = E/E_e$, $\lambda = \gamma^2\phi^2$, and $\eta = (1 + \lambda)^{-2}$. Eq. (1) is known to overestimate the muon pair production by a factor of two.

The number of muons per electron accepted in an angle $\leq \phi$, in a momentum bite of $\pm \Delta p/p$ at a muon energy E is

$$A_\mu = \left[\frac{\mathrm{d}F}{\mathrm{d}E}(E_e, E, 0) - \frac{\mathrm{d}F}{\mathrm{d}E}(E_e, E, \phi) \right] E \frac{2\Delta p}{p}. \quad (2)$$

From Eq. (2) it is immediately obvious that one will prefer to accept muons with a large value of E/E_e rather than with a small E/E_e as long as the function $\mathrm{d}F/\mathrm{d}E$ is relatively flat in energy. For small muon production angles this condition obtains for the energy range, $0.2 < E/E_e < 0.8$. The same consideration also argues that one should choose a large initial electron beam energy. Figs. 2a and 2b display plots of Eq. (2) for a low energy and a high energy production option respectively.

At the front surface of the production target the electron beam can be focused to a spot of radius, $r_b \approx 1$ mm. The muons will, however, appear to originate from a somewhat larger spot with a size given by the radial extent of the electromagnetic shower at a depth corresponding to the shower maximum, which occurs approximately six radiation lengths $(6X_0)$ inside the target. The radiation length, X_0, for tungsten is 3 mm; hence the shower maximum will occur at ≈ -20 mm, and a tungsten target

30 mm long will yield almost the entire thick target conversion to muons.

At the depth corresponding to the shower maximum the primary electron beam will have suffered a mean scattering angle of

$$\Theta^2 = \left(\frac{0.028 \text{ GeV}}{E_e} \right)^2 \left(\frac{6X_0}{X_0} \right), \quad (3)$$

which will induce a radial spread of $6X_0\Theta$ in the primary beam. Actually in a high Z target, the shower will spread by an amount roughly double this value. Hence, the shower radius can be approximated by

$$r_{sh} = \left(r_b^2 + (12\Theta X_0)^2 \right)^{1/2}. \quad (4)$$

At production the geometrical emittance, $\epsilon(E)$, of the muon beam of energy, E, accepted into an angle ϕ_{accept} will be

$$\epsilon(E) = \frac{\epsilon_{n,prod}}{\gamma_{prod}} = r_{sh}\phi_{accept}, \quad (5)$$

where $\epsilon_{n,prod}$ is the normalized emittance at production.

To increase the muon production efficiency one might consider alternate techniques of photo-production. The production process consists of two steps: 1) conversion of the electron energy into photons and 2) muon pair production from the photons. Rather than using bremsstrahlung, one might employ synchrotron radiation as the conversion process. Synchrotron radiation conversion could either take place in a crystal or in a plasma [4], which has an obvious advantage of being more amenable to high average power operation.

The choice of synchrotron radiation conversion is unlikely to increase the rate of muon production as the mean photon energy is lower for the synchrotron radiation photons than for the bremsstrahlung photons. The synchrotron radiation photons are more numerous, but only at low energies for which muon pair production is not energetically allowed. The angular distribution of the muons produced will be dominated by the spread of angles of the electrons in the primary beam as the average electron angle will be significantly larger than γ^{-1}.

The pair production rate in crystals is known experimentally [5] to be larger than in amorphous materials due to the coherent field effects. For photons of 100 GeV, the coherent production is a few times the Bethe–Heitler rate; however, for 20 GeV photons this effect increases pair production by only 10%. As the mean energy of bremsstrahlung photons is $\approx 20\%$ of the incident beam energy, pair production in a crystal will not significantly enhance the muon yield for a 100 GeV per beam collider. Hence, in the analysis that follows we restrict our attention to the use of a conversion bremsstrahlung production target.

3. Ionization cooling

In designing a collider one will inevitably seek a means of having as low an emittance as possible for the beams. One suggested means of cooling the muons (Fig. 3) is to pass the beam through a succession of alternating slabs of material (ionization cells) and rf-accelerating sections. In the ionization cells each of the muons gives up momentum along its particular trajectory, thereby losing transverse and longitudinal momentum. In the accelerating sections the longitudinal momentum is restored to the beam. Thus the transverse emittance of the beam is reduced in a manner analogous to radiation damping.

Neuffer [6] has shown that the ionization cooling of the transverse emittance is limited by beam heating due to multiple Coulomb scattering. If the transverse cooling is performed at an energy, E_c, using a medium for which the radiation length is X_R and the ionization loss rate is dE/dx, then the equilibrium, normalized emittance will be

$$\epsilon_{eq,n} = \frac{\beta_{cool}}{2} \frac{(14\ \text{MeV})^2}{m_\mu c^2 \left(X_R \dfrac{dE}{dx} \right)}, \tag{6}$$

where β_{cool} is the value of the beta function in the scattering medium. From Eq. (6) it follows that efficient cooling requires that one employ a very strong focusing system that brings the beam to a symmetric waste of small radius in the ionization medium. For high energy muons traversing a medium of density ρ (g/cm^3), of atomic number Z, and of atomic weight, A, the ionization loss rate can be approximated [7] by

$$\frac{dE}{dx} = \frac{DZ\rho}{A\beta^2} \left\{ \ln\left(\frac{2m_e \gamma^2 \beta^2 c^2}{I} - \beta^2 \right) \right\}, \tag{7}$$

where $\beta = v/c$, $D = 0.307$ and $I = 16Z^{0.9}$ eV. For materials with $Z \geq 6$, the radiation length may be approximated by

$$X_R(\text{cm}) = \frac{716.4 A}{\rho Z(Z+1) \ln(287 Z^{-1/2})}. \tag{8}$$

Multiplying Eqs. (7) and (8), one observes that the product $(X_R\ dE/dx)$ is independent of the density of the ionization medium and is greatest for small values of Z. Hence,
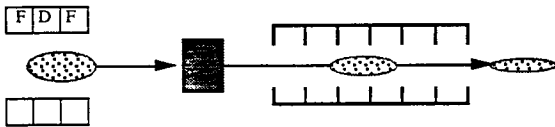

Fig. 3. Schematic of the basic components of an ionization cooling array: a strong lens to focus the beam, the ionization medium in which the particles lose both transverse and longitudinal momentum, and an accelerating structure to restore the longitudinal momentum of the beam.
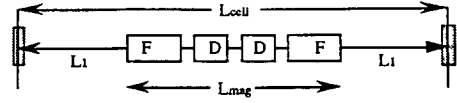

Fig. 4. Schematic of the triplet optics of an ionization cooling cell; the disks of the ionizing medium are shaded and have a half width of $\beta_{cool}/4$.

low Z media will be preferred over high Z media for ionization cooling. The length of the scattering medium in any individual ionization cell will have to be limited to $\beta_{cool}/2$.

As the momentum bite of the selected muons will be relatively large, one should consider using optics with second order chromatic corrections to focus the beam onto the ionization targets as otherwise the spot size will be unacceptably large. The focusing system may be a strong quadrupole triplet. Brown [8] has suggested a focal system that is suitable for scaling calculations. In this triplet transverse dimensions are scaled by a factor a_q, which is the aperture (radius) of the first quadrupole of the triplet; longitudinal dimensions are scaled by the "ideal" focal length, f,

$$f = \left(\frac{a_q}{B_q} (B\rho) \right)^{1/2}, \tag{9}$$

where B_q is the pole tip field in the first quadrupole, and $(B\rho)$ is the magnetic rigidity of the beam. For a beam of momentum p,

$$B(\text{T})\rho(\text{m}) = 3.3 p(\text{GeV}/c)c. \tag{10}$$

The optical invariants of this particular triplet design are incorporated into the scaling equations that follow; the geometry of the design is illustrated in Fig. 4.

The free space from the focus to the first quadrupole, L_1, is $1.36f$; the length of the triplet, L_{mag}, is $3.13f$ and the length of the cooling cell, l_{cell} is $5.85f$. Without chromatic correction the value of β_{cool} for a beam with fractional momentum spread $\sigma_p(= \Delta p/p)$ is given by

$$\beta_{cool} = 5.92 \sigma_p f. \tag{11}$$

With second order chromatic correction of the focusing optics the beta function can be reduced to

$$\beta_{cool} = 74.0(B\rho) \left(\frac{a_q}{f B_q} \right) \sigma_p^2. \tag{12}$$

In the analysis that follows we chose the corrected optics described by Eq. (12). As the cooling disks have a length, $\beta_{cool}/2$, each cooling cell produces an energy loss of e_{cell}, limited to

$$e_{cell} = \frac{\beta_{cool}}{2} \frac{dE}{dx}. \tag{13}$$

In optimizing the production/cooling scenario for the muon collider, one can now choose both the energy of

muon production, E_μ, and the energy at which the cooling is performed, E_c. Note that although the equilibrium emittance of Eq. (6) does not depend explicitly on the cooling energy, the choice of E_μ, E_c, and the momentum acceptance will determine σ_p and thereby β_{cool} in the cooling lattice. Thus the choice of E_c will determine the transverse cooling coefficient, C_μ, via

$$C_\mu = \frac{\epsilon_{n,prod}}{\epsilon_{eq,n}} = \frac{r_{sh}\phi_{accept}\gamma_{prod}}{\epsilon_{eq,n}}. \tag{14}$$

The choice of E_μ will also influence the number of muons per bunch that are available to be injected into the collider as some of the muons will decay as they traverse the cooling lattice. If energy is replaced during the cooling process by accelerator cells with an average accelerating gradient G, the total path length in the cooling lattice, L_{cool}, will be

$$L_{cool} = \frac{E_c}{F_c}\left(\frac{L_{cell}}{e_{cool}} + \frac{1}{G}\right) \ln(C_\mu). \tag{15}$$

In Eq. (15) F_c is the overall packing fraction of the ionization and acceleration cells in the cooler lattice. F_c accounts for pumping ports, flanges, diagnostics, bending magnets, and sextupoles in the cooling lattice. If the number of muons per bunch that is injected into the cooling lattice is N_μ, then the number of muons per bunch available for injection into the collider will be

$$N_\mu^* = N_\mu \exp\left(-\frac{L_{cool}}{c\tau_\mu\gamma_c}\right), \tag{16}$$

where τ_μ is the muon lifetime at rest, and γ_c is $E_c/m_\mu c^2$.

Longitudinal cooling of the beam would allow smaller values of β_{cool} and consequently lower equilibrium emittances. Such reduction of the momentum spread can be accomplished by two means: 1) adiabatic damping by accelerating the muons prior to transverse cooling and 2) ionization cooling either in the transverse damper or in a separate damping structure. If the longitudinal cooling were limited to the ionization damping in the zero-dispersion cells of the transverse damper described above, the amount of acceleration, A_μ needed [4] to reduce the momentum spread by a factor $1/e$ would be

$$A_\mu = E_c\left(\frac{dE/dx}{E_c\dfrac{\partial^2 E}{\partial E_\mu \partial x}}\right) \approx 5E_c. \tag{17}$$

If the longitudinal cooling is done in a dispersive section, the energy spread might be reduced by $1/e$ with as little as $2E_c$ of total energy exchange.

As computed from Eq. (16), the path length of the muons in the cooler will typically be tens of kilometers, even if the packing fraction of the cooling lattice is large. A large packing fraction in conjunction with a high muon
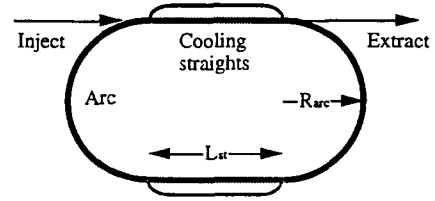

Fig. 5. A 2-in-1 muon cooling ring. Transverse coolers are in each of the straight sections. The gray sections have large aperture quadrupoles for the first stage of cooling; the black straights have stronger, small aperture quadrupoles.

energy implies that the transverse emittance cooler should be constructed in the form of a recirculating linac such as CEBAF with high field bending magnets in the arcs and with as much as a few GeV per turn of acceleration in the straight, cooling sections.

At injection into the cooler the transverse emittance and the momentum spread of the muon beam will be large. Consequently the apertures of the quadrupoles in the cooling straights must be relatively large. One may envision a more effective form of cooler in which the emittance is reduced by an order of magnitude before injection into a final cooler which can have stronger, smaller aperture quadrupoles. As the value of β_{cool} can be much smaller in the second cooler, the equilibrium emittance could be much smaller than achievable in a single cooling ring. In such a scheme there is no need to duplicate the cost of the high field, dipole arcs. Rather the two coolers can share common arcs in a 2-in-1 arrangement illustrated in Fig. 5. The choice of straight-through or by-pass paths for the cooling stages can be selected to minimize the total path length of the muons in the coolers.

In the cooling ring the total length of the cooling cells plus re-acceleration cavities is $2L_{st}P_c$ where P_c is the packing fraction of ionization cells plus accelerator cells in the straight sections. As the overall packing fraction, F_c, is just $[2L_{st}P_c(2\pi R_{arc} + 2L_{st})^{-1}]$, the number of cooling cells, N_c is related to the average dipole field in the bends, $\langle B_d\rangle$ and the accelerating field, G, by

$$N_c = F_c\frac{2\pi(B\rho)}{\langle B_d\rangle}\left[1 - \frac{F_c}{P_c}\right]^{-1}\left[l_{cell} + \frac{e_{cell}}{G}\right]^{-1}. \tag{18}$$

Hence, the rf-system of the cooling ring must supply $N_c e_{cell}$ volts per turn. In damping the emittance of the muons by a factor C_μ, the muons must execute $[E_c N_c e_{cell}^{-1} \ln C_\mu]$ turns.

4. Collider considerations

The number of muons per bunch. N_μ^*, that circulate in the collider will be determined by the production efficiency, A_μ, by the charge, N_e in the electron bunch that

strikes the production target, and by the path length through the cooling lattice. The number of electrons per bunch will be limited by the beam loading in the linac and by the design of the electron gun. The present SLAC gun (thermionic) produces bunches of 10 nC. If the electron beam emittance is not critical, the charge in the electron bunch can be raised to 20–30 nC. Bunches with as much as 50 nC may be produced with a photocathode gun, but such a large charge would lead to large beam loading and complications form the beam-breakup instability in an S-band linear accelerator.

The electron bunches will be produced in a macropulse of duration, τ_e, which is chosen to match the circulation period of the muons in the storage ring collider (Fig. 1). If the average dipole field in the ring is 3 T and if the muon energy is 100 GeV, then the circulation period will be 2 μs:

$$\tau_e = 2\mu s \times \left(\frac{3\,T}{B_{ave}}\right)\left(\frac{E_\mu}{100\,GeV}\right). \qquad (19)$$

If the number of bunches per macropulse is N_b, then the frequency of collisions in the collider will be

$$f_{coll} = N_b/\tau_e. \qquad (20)$$

To maintain the muon population in the collider the linac must be pulsed at a frequency of τ_μ^{-1}, where τ_μ is the muon lifetime as seen in the laboratory; at 100 GeV. $\tau_\mu = 2$ ms. Hence, the duty factor of the linac will be τ_e/τ_μ. The average power of the electron beam on the muon production target is, therefore,

$$P_{beam} = q\frac{N_b N_e}{\tau_e}\frac{\tau_e}{\tau_\mu}E_e = q\frac{N_b N_e}{\tau_\mu}E_e, \qquad (21)$$

where q is the electron charge.

The peak luminosity of the collider with muons with a geometrical emittance, ϵ, can be written as

$$L = \frac{N_\mu^* f_{coll}}{4\pi\epsilon\beta^*}, \qquad (22)$$

where $\gamma = E_\mu/\mu$ and β^* is the value of the beta function at the collision point. Combining Eqs. (5), (16), (20) and (22), and evaluating the average luminosity of a collider of repetition rate, R, we obtain the following expression for the average luminosity of the collider,

$$\langle L \rangle = \frac{A_\mu^2 N_e^2 N_b \gamma C_\mu}{4\pi r_{sh}\phi_{accept}\beta^*\tau_e}\left(\frac{\gamma}{\gamma_{prod}}\right)\exp\left(-\frac{2L_{cool}}{c\tau_\mu\gamma_c}\right)$$

$$\times \left[1 - \exp\left(\frac{2}{\tau_\mu\gamma R}\right)\right]\left(\frac{\tau_\mu\gamma R}{2}\right), \qquad (21)$$

The factor, γ/γ_{prod}, implies that maximizing the luminosity argues for accepting the muons into the muon linac at an energy somewhat lower than the energy which maximizes A_μ. The factor, C_μ, accounts for the possibility of cooling the muons; if no transverse cooling is used, $C_\mu = 1$

and $L_{cool} = 0$. At 100 GeV a reasonable value of β^* can be assumed to be 1 cm, although smaller values are possible, limited by the muon bunch length and by the design of the detector. Hence, the length of the muon bunch should be less than 1 cm. Such a short pulse is assured, if the length of the electron beam pulses are ≈ 0.5 cm.

5. Examples and parametric dependences

One now has a complete set of equations with which to maximize the luminosity of the muon collider as a function of the electron beam power incident on the production target and other system characteristics. As a first step in examining parametric dependences, we formulate a "realistic", baseline scenario that does not employ cooling of the muon beam.

The CLIC group at CERN [9] has developed a design concept for a high power positron production target to operate at 500 to 750 kW, more than an order of magnitude greater than presently operating designs. For the "realistic", baseline scenario assume that this target design can be realized at 0.5 MW. Using a 50 GeV electron beam with 20 nC per bunch and one bunch per macropulse, one can produce muon bunches of ≈ 0.1 nC at 29 GeV with an acceptance of $\pm 3\%$ in the capture section of the muon linac. The geometrical emittance of the muon beam at 29 GeV will be 5 π mm-mrad. If the average dipole field in the collider is 3 T, the revolution period will be 2 μs. Hence, the collision frequency will be ≈ 0.5 MHz. Then for β^* equal to 1 cm, the luminosity of the muon collider at 100 GeV will be $\approx 2 \times 10^{26}$ cm^{-2}s^{-1}. This scenario, which we will use as a base case for parametric studies, is summarized as column 1 in Table 1 along with a more optimistic case without cooling (column 3).

The improvements to the "realistic" and " optimistic" cases that would obtain from damping the transverse emittance of the muons via ionization cooling are shown in columns 2 and 4 respectively. A far more optimistic scenario (column 5), which also requires several technological inventions including considerable cooling of the muon beam, is discussed in Section 6. In all the examples with beam cooling the ionization media are beryllium disks of thickness of $\beta_{cool}/2$. The beam is re-accelerated in rf-cavities with rf-cavities operating with an average accelerating gradient of 17 MeV/m.

The effect of the choice of the electron beam energy on the production efficiency can be seen in Fig. 6, which displays the maximum luminosity versus the electron beam energy for the realistic scenario. In this calculation the number of electron bunches is varied to keep the beam power on the muon production target fixed at 0.5 MW. The momentum acceptance is fixed at $\pm 3\%$; however, the value of muon energy accepted and the angular spread of muons accepted is varied so as to maximize the luminos-

Table 1

Characteristics of a 100 GeV × 100 GeV muon collider using electro-production. The repetition rate in all cases is 500 Hz. For multiple rings, B_q, a_q, β_{cool} refer to the second ring. The quantities with daggers require technological inventions

	"Realistic" no cooling	"Realistic" with cooling	"Optimistic" no cooling	"Optimistic" with cooling	Needs inventions
Production					
E_e (GeV)	50	50	50	50	50
P_{beam} (MW)	0.5	0.5	2	2	5 †
N_e (nC)	20	20	30	30	50 †
F_{accent} (GeV)	29	21	29	22	25
$(\Delta p/p)_u$(%)	±3	±3	±4	±4	±8
N_u (nC)	0.1	0.1	0.2	0.18	0.6
ϵ_n (π m rad)	1.95×10^{-3}	2.2×10^{-3}	1.95×10^{-3}	2.2×10^{-3}	3.0×10^{-3}
Cooler					
E_{cool} (GeV)	–	40	–	45	100 †
Number of rings	0	1	0	1	2
F_{cool}	–	0.5	–	0.5	0.6
$\langle B_d \rangle$ in (arc) (T)	–	4.5	–	4.5	4.5
V_{ring} (GeV/turn)	–	0.95	–	1.2	3.2
C_{ring} (m)	–	491	–	553	1840
(B_q (T), a_q (cm))	–	(4, 1.5)	–	(6, 1.2)	(8†, 0.5)
β_{cool} (cm)	–	1.3	–	1.5	0.4
ϵ_{med} (π m rad)	1.7×10^{-3}	5.7×10^{-5}	1.9×10^{-3}	7.4×10^{-5}	1.6×10^{-5}
C_u	1	38	1	28	136
Collider					
N_u (nC)	0.1	0.068	0.2	0.14	0.35
N_{bunch}	1	1	2	2	2
B_{ave} (T)	3	3	4.5	4.5	6 †
$C_{collider}$ (m)	690	690	460	460	345
f_{coll} (MHz)	0.5	0.5	1.33	1.33	2
β (cm)	1	1	1	1	0.4
$(\Delta E/E)_{collider}$ (%)	±0.9	±0.8	±1.3	±1.0	±0.6
$\langle L \rangle$ (cm^{-2} s^{-1})	1.5×10^{26}	9.5×10^{26}	7.1×10^{26}	8.6×10^{27}	1.0×10^{30}

ity. As can be seen from Eqs. (2) and (22), the optimum acceptance energy will be a large fraction of the beam energy as the luminosity is quadratic in the conversion efficiency.

The scenarios employing production of muons at high initial energy (20–30 GeV) achieve relatively high lumi-
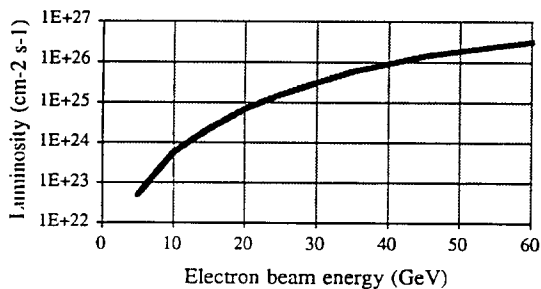

Fig. 6. The variation of collider luminosity with energy of the electron beam at the production target in the "realistic" scenario. The beam power is fixed at 0.5 MW.

nosity at the expense of producing a muon beam with a relatively large ($\approx 1\%$) momentum spread at the interaction point. If a much lower spread, say ±0.1%, were required for physics reasons, then the accepted muon energy, E_{accept}, would have to be reduced to ≈ 5 GeV. The luminosity is still maximized by maximizing the electron beam energy. Making this change in E_{accept} to the "realistic" scenario reduces the luminosity to $\approx 6 \times 10^{24}$ cm^{-2}s^{-1}. As transverse cooling is accompanied by damping of the momentum spread, this consideration is not as severe in the scenarios with beam cooling.

The optimum energy for accepting the muons in the absence of cooling is 29 GeV. If instead we employ an ionization cooler, the optimum acceptance energy would be reduced to 21 GeV; a curve of the luminosity versus muon acceptance energy for the "realistic scenario" is given in Fig. 7. In this calculation cooling energy has been optimized but limited to ≤ 40 GeV.

Somewhat surprisingly, the higher the energy at which the muons are cooled, the higher the final luminosity. The reason is that the adiabatic damping of the energy spread permits a much smaller value of β_c. If an initial stage of
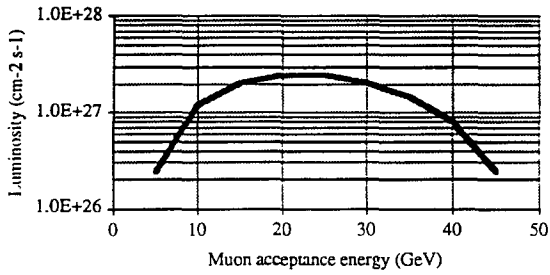
Fig. 7. Luminosity as a function of muon acceptance energy for the "realistic" scenario with ionization cooling.
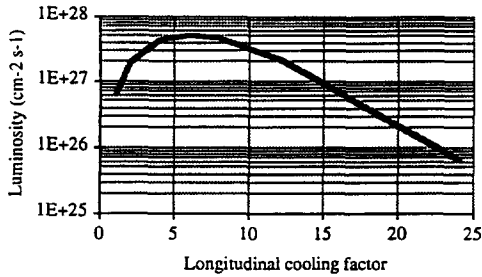

Fig. 8. Luminosity variation with longitudinal cooling for the "realistic" scenario.
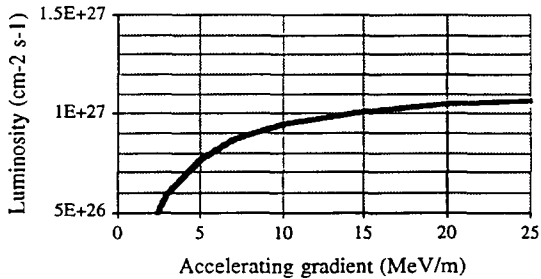

Fig. 9. Luminosity versus accelerating field in the cooling ring for the "realistic" scenario of Table 1.
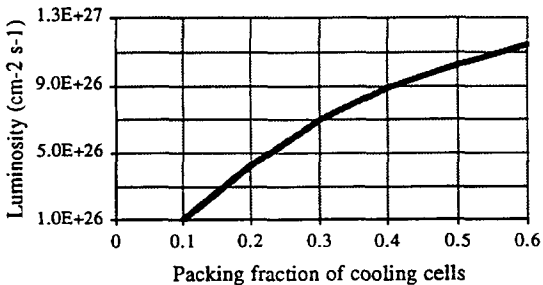

Fig. 10. Luminosity versus packing fraction of ionization cells and re-acceleration cavities in the cooling ring for the "realistic" scenario of Table 1.

Fig. 11. Variation of luminosity with the choice of ionizing medium.

ionization cooling were employed to reduce the energy spread, the optimum energy at which transverse cooling is performed could shift to a lower value. In the "realistic" example, the traverse cooling by a factor of 48 at 40 GeV requires an energy exchange of only $3.8E_c$. From Eq. (17) one expects a slight improvement in C_μ from the damping of the energy spread in the zero-dispersion cells. Adding ionization cells in the dispersive sections of the ring as suggested in Ref. [6] could improve the luminosity significantly.

Fig. 8 illustrates the variation in luminosity for the "realistic" scenario with longitudinal cooling accompanying the transverse emittance damping. In this calculation cooling is done at the muon acceptance energy, 21 GeV so that no additional adiabatic reduction in energy spread is included. The field strength and aperture of the cooling channel optics is kept fixed. The decrease in luminosity as the cooling factor increases beyond six comes from the decay of the muon population as the transverse cooling path length increases to allow the beam to reach the equilibrium emittance.

As the muons must remain in the cooling lattice for hundreds of microseconds, it may not be possible to maintain an accelerating gradient of 17 MeV/m as assumed in the examples of Table 1. The consequence of reducing the gradient to allow for a lower power accelerating system in the cooling ring is displayed in Fig. 9. The degradation of the luminosity becomes especially large as the gradient falls below 10 MeV/m. As the number of muons in the ring is small, the beam loading in the cooling ring will be very small. One might consider the use of superconducting rf-cavities to keep rf-power requirements relatively small. Whether the superconducting cavities can function in the presence of radiation from the muon decay is uncertain.

A second characteristic of the ionization cooling lattice that can have a strong effect on the final luminosity of the collider is the packing fraction, F_c, of the ionization cells plus the rf-cavities in the cooling ring. Fig. 10 illustrates the variation of luminosity with F_c for the "realistic" case with cooling.
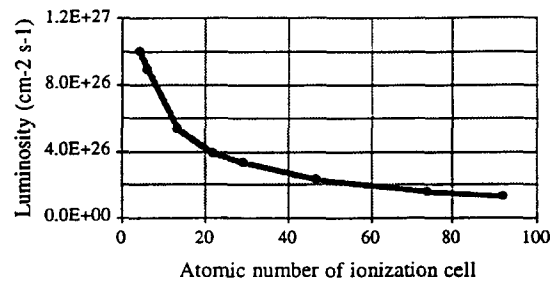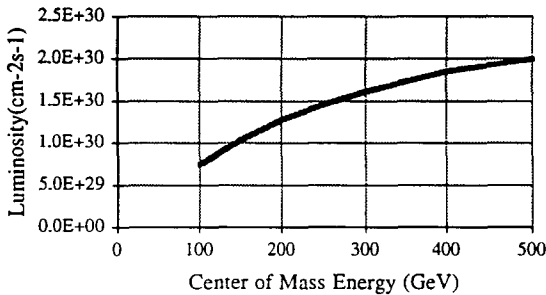
Fig. 12. Variation of luminosity with energy for a 250 GeV × 250 GeV muon collider with $\beta^* = 0.3$ cm.

Applying Eq. (7) through Eq. (17) to calculate the characteristics of a cooling system, we find that the luminosity varies with choice of the ionizing medium as shown in Fig. 11. Although the product X_R dE/dx is independent of density, the luminosity is sensitive to the density of the ionizing medium as the energy lost per cell depends on the density and thickness of the medium. For each of the points in Fig. 11 the appropriate density has been used. From this examination we confirm that the preferred ionization media are beryllium disks.

If one were to design the muon collider with a broader energy reach, for example from 100 to 500 GeV center of mass energy, one would hope to realize a higher luminosity at the higher energies as the geometrical emittance is reduced by adiabatic damping. The scaling of the luminosity, as shown in Fig. 12, is slower than linear. The calculation of Fig. 12 is based on the "Needs invention" scenario of Table 1, with β^* reduced to 0.3 cm.

In this scenario the momentum spread of the beams is largest at the lowest energy. Unfortunately, the width of a Standard Model Higgs is expected to be a rapidly increasing function of the Higgs mass with a value of 1 GeV/c^2 for $m_H = 100$ GeV/c^2. If the momentum spread were reduced at the lower energies to allow for a fine scan of the range from 100 to 200 GeV, the luminosity would fall off much more precipitously.

6. Prospects and conclusions

To obtain a muon collider with a luminosity of 10^{30} cm^{-2}s^{-1}, as desired for studies of the Higgs, one must adopt an extremely optimistic scenario (column 5 of Table 1) that includes several technological innovations (indicated by a dagger). Perhaps the easiest of these advances may be the development of very strong, precision dipoles that would enable one to design a relatively small storage ring collider with a dipole field of 6 T averaged over the entire ring.

Continuing advances in the technology of electron guns with photocathodes suggest that one may be able to obtain 50 nC bunches of electrons for injection in a S-band

structure. Accelerating multiple bunches of such high charge in a S-band structure also presents difficulties. For a 50 nC, 15 ps bunch, the single-bunch beam loading in a SLAC structure operating at 20 MeV/m would be ≈ 20%. As the bunches in the macropulse are separated by hundreds of meters, multi-bunch beam breakup is not a problem. However, a head-to-tail momentum variation of 4% will be required for BNS damping of the single bunch, transverse, head-to-tail instability. Once this systematic variation is removed at the end of the electron linac, one would be left with a ± 1.5% spread that must be handled by the focusing optics at the production target.

Extending the conceptual design of the CERN production target to a reliable, 5 MW design is likely to be very difficult. Of particular difficulty will be finding suitable accelerator components that can withstand the extremely high radiation environment near the target. Note that the highest power, production target in operation is the 33 kW positron production target at SLAC.

It is likely that the greatest challenge to the designer will be to find an efficient scheme for cooling the muon beam at a high initial energy. In scenarios that include beam cooling in a storage ring the momentum bite must be chosen to be consistent with the acceptance of the cooling lattice. As it should be possible to design a lattice with an acceptance of ± 2%, cooling the muons at very high energy allows accepting a large momentum bite at the production target.

An idea of the scope of the project can be had by observing that in the realistic case the collider ring (as a circumference of ≈ 690 m while the cooler rings , one each for the μ^+ and μ^-) have circumferences of ≈ 90 m. Operating with a gradient of 17 MeV/m, the electron linac would be 3 km long while the 20 GeV muon linac would have a length of 1.32 km. A clever design may be possible in which these same linacs could be used to accelerate the muons from the cooler ring up to the full 100 GeV per beam of the collider. In this case the major cost of the project would be the 70 GeV of S-band linac. The major complexity and technological risk is in the lattices of the cooling rings which use very high field, superconducting quadrupoles and dipoles.

In conclusion, one sees that even with optimistic assumptions, it is difficult to envision a high energy $\mu^+\mu^-$ collider which employs electro-production of muons functioning with a luminosity $> 10^{27}$ cm^{-2}s^{-1}. While the possibility of an electron-beam-driven muon collider with a luminosity ≈ 10^{30} cm^{-2}s^{-1} cannot be ruled out, it would require major advances in several of the primary constituent technologies. The areas for innovations include superconducting dipoles and quadrupoles, multi-kiloampere electron beam sources, and multi-megawatt muon production targets. Most critically, efficient means of both transverse and longitudinal of cooling the muon beams at high energy must be found and demonstrated, if suitably high luminosity is to be achieved.

References

[1] D.B. Cline, Opening presentation at the Workshop on High Energy Muon Colliders, Napa, California, December, 1992.

[2] W.R. Nelson, K.R. Case and G.K. Svensson, Nucl. Instr. and Meth. 120 (1974) 413.

[3] W.R. Nelson, Nucl. Instr. and Meth. 66 (1968) 293.

[4] W.A. Barletta, and A.M. Sessler, Radiation from fine self-focussed beams at high energy, in: High Gain, High Power Free Electron Lasers; eds. L. Bonifacio, L. De Salvo-Souza and C. Pellegrini (Elsevier, 1989).

[5] A. Belkacem et al., Experimental study of pair creation and radiation in Ge crystals at ultra-relativistic energies, in: Relativistic Channeling., eds. Carrigan and Ellison, Nato ASI Series B, Vol. 165 (Plenum).

[6] D. Neuffer, Part. Accel. 14 (1983) 75.

[7] Particle Data Group, Phys. Rev. D45 Part 2 (1992).

[8] K. Brown, Private communication as reported in R. Palmer, Interdependence of Parameters for TeV Linear Colliders, Proc. Workshop on New Developments in Particle Accelerator Techniques, Orsay, (June 1987).

[9] P. Sievers, Proc. Workshop on Heavy Quark Factories, Courmayeur, Italy, December, 1987.